

Transtemporal investigation of brain parenchyma elasticity using 2-D shear wave elastography: definition of age-matched normal values

Michael Ertl, Nele Raasch, Gertrud Hammel, Katharina Harter, Christopher Lang

Angaben zur Veröffentlichung / Publication details:

Ertl, Michael, Nele Raasch, Gertrud Hammel, Katharina Harter, and Christopher Lang. 2018. "Transtemporal investigation of brain parenchyma elasticity using 2-D shear wave elastography: definition of age-matched normal values." *Ultrasound in Medicine & Biology* 44 (1): 78–84. <https://doi.org/10.1016/j.ultrasmedbio.2017.08.1885>.

TRANSTEMPORAL INVESTIGATION OF BRAIN PARENCHYMA ELASTICITY USING 2-D SHEAR WAVE ELASTOGRAPHY: DEFINITION OF AGE-MATCHED NORMAL VALUES

MICHAEL ERTL,^{*} NELE RAASCH,^{*} GERTRUD HAMMEL,^{†,‡} KATHARINA HARTER,^{†,‡} and CHRISTOPHER LANG^{*}

^{*} Clinic for Neurology and Neurophysiology, Klinikum Augsburg, Augsburg, Germany; [†] Chair and Institute of Environmental Medicine, UNIKA-T, Technical University of Munich and Helmholtz Zentrum München, Germany - German Research Center for Environmental Health, Augsburg, Germany; and [‡] CK-CARE, Christine Kühne - Center for Allergy and Research and Education, Davos, Switzerland

INTRODUCTION

Ultrasonographic shear wave elastography measures local tissue stiffness, analyzing ultrasound-induced shear wave propagation. The ultrasound probe generates a localized radiation force, which induces shear waves that propagate from that focal point directly in the tissue of interest. Propagation speed of shear waves is directly related to the elasticity of tissues. This propagation is slower in soft tissue than in a stiff region (Bamber et al. 2013). This technique is already used in a variety of medical disciplines: to determine the grade of liver cirrhosis (Sandrin et al. 2003); in the staging of prostate carcinomas (Sarvazyan et al. 2011); or in the investigation of various pathologies of the thyroid gland (Vorlander et al. 2010), the lymph nodes (Xu et al. 2011) or the breast parenchyma (Garra et al. 1997).

The importance of brain parenchyma elastography has been evaluated in various types of brain pathologies—for example, neoplastic (Shiroishi et al. 2016), inflammatory (Enzinger et al. 2015) or degenerative (Wang et al. 2013) processes—using magnetic resonance elastography, although data about ultrasound elastography remain scarce. A few studies have investigated brain tissue elasticity by ultrasound brain parenchyma elastography (uBPE), mainly in the neurosurgical field, where various entities of brain tumors (*e.g.*, meningiomas, low-grade gliomas, high-grade gliomas and metastases) were studied intra-operatively (Chauvet et al. 2016), with the surrounding bone having been removed earlier. These preconditions lead to a restriction in applicability for patients in need of surgery. Recently, normal values were established from various brain regions of neonates, applying the slightly different approach of acoustic radiation force impulse imaging. Of course, the neonates were examined *via* the fontanelles without the obstruction caused by the skull. Values were dependent on age and brain region (Su et al. 2015).

Address correspondence to: Michael Ertl, Clinic for Neurology and Neurophysiology, Klinikum Augsburg, Stenglinstr. 2, 86156 Augsburg, Germany. E-mail: Michael.Ertl@klinikum-augsburg.de

To the best of our knowledge, no scientific findings report the possibility of reliable investigation on brain tissue, applying uBPE in the presence of an intact skull. Few, but encouraging, data are available from animal research (Xu et al. 2013), with values of healthy brain tissue ranging 4.32–4.49 kPa.

The objective of this study was to evaluate whether brain parenchyma elasticity can be measured reliably in persons with an intact temporal bone. Possible applications of uBPE might be the preclinical discrimination of hemorrhagic and ischemic strokes to accelerate clot-dissolving therapy according to the *time is brain* concept and the evaluation of the compression of vital brain tissue by mass lesions, such as intra-cerebral bleedings.

MATERIALS AND METHODS

The study protocol was approved by the medical institutional review board at the Clinic of Augsburg (No 2016-23) in accordance with the guidelines of the Declaration of Helsinki. All patients or their legal representatives provided written informed consent before enrollment.

Study population

Between September 2016 and March 2017, patients and healthy volunteers were enrolled in this prospective study. In total, 108 subjects were examined. For patient inclusion, the presence of a relevant intra-cranial pathology had to be excluded by sufficient cerebral imaging (computed tomography [CT] or magnet resonance imaging [MRI]). Only patients with exclusively peripheral neurological symptoms were eligible. We recruited 11 patients. Their diagnoses and numbers were as follows: benign paroxysmal positional vertigo ($n = 3$), vestibular neuritis ($n = 1$), Guillain-Barré-syndrome ($n = 2$), Miller-Fisher-syndrome ($n = 1$), myopathy ($n = 1$), thoracic-outlet syndrome ($n = 1$) and conversion disorder ($n = 2$). Not included in the study were 3 patients with confirmed hemorrhagic ($n = 1$) and ischemic ($n = 2$) stroke. They were used as examples for values in damaged brain tissue. Neuroimaging evaluations were conducted by specialized neuroradiologists.

Transtemporal ultrasound brain parenchyma elastography

For ultrasound examination a 1.5–4.4 MHz convex ultrasound transducer (Model C5-1, Philips, Amsterdam, Netherlands), normally used for abdominal ultrasound, was employed because our standard sector transducers, normally used for transcranial ultrasound, were not equipped for tissue elastography analysis. For shear wave elastography, the specific mode of the Philips iU22 machine was applied. The transducer was placed on the temporal margin of the patient's skull for evaluation of the transtemporal bone window. In the presence of a proper bone window, the usual landmarks for identification of the midbrain plane were

clearly visible. Elastography measurements (EMs) were only performed if all the relevant landmarks for the identification (*e.g.*, visualization of the midbrain peduncles) were on display. Patients with no proper bone window were excluded from the study. B-mode and shear wave elastography images were acquired bilaterally, if possible.

To ensure exact and reproducible measurements of brain parenchyma, a standardized examination depth of 3–4 cm in the midbrain plane was defined to gain information about subcortical brain tissue. This region was selected because it was most easily accessible through the transtemporal bone window. During data acquisition, patients were asked to hold their breath to ensure as few artifacts as possible. For EMs, a box with fixed dimensions of 1.0×0.5 cm was used, predefined in the elastography settings of the ultrasound machine.

In every case, measurements were either performed by a single experienced examiner accredited by the German Medical Ultrasound Society or supervised by this specialist. To reduce measuring intolerances, the examination was repeated at least two times by the same examiner. For illustration of exemplary values in damaged brain tissue (three patients), EM was also performed in regions of ischemic and hemorrhagic strokes, predefined by alternative imaging (CT).

Safety considerations

As noted earlier, 2-D shear wave elastography is already in widespread use for other parenchymatous organs without any relevant risks and is recommended by the respective guidelines (Barr et al. 2015, 2017; Cosgrove et al. 2017; Ferraioli et al. 2015; Shiina et al. 2015). Additionally, reliable data for the use in brain tissue were supplied by experimental animal studies (Li et al. 2016). No adverse effects were reported in neurosurgical investigations with the protective skull having been removed (Chauvet et al. 2016). Investigations were performed according to the *as low as reasonably achievable* (ALARA)-radiation safety principle (Toms 2006).

Statistical analysis

Statistical analysis was performed, using SAS 9.4 (SAS Institute, Inc., Cary, NC, USA). As not all patients had a sufficient temporal bone window on both sides, there were 9 patients who could only be investigated unilaterally. These patients were included with the available data. Structural equality of patients evaluated by each investigator were compared with respect to sex and age group (20–40 y, 40–60 y and >60 y), using a Chi-square test. Age and body mass index (BMI) were analyzed using *t*-tests, and Pearson's correlation coefficient was used for showing correlation of age and BMI with EM values. Possible influence of the sequence and the side of measurements were evaluated by a mixed model for

Table 1. Characteristics of the study population

		N	%	
All		108	100.00	
Sex	female	64	59.26	
	male	44	40.74	
Age group	20–39 y	40	37.04	
	40–59 y	40	37.04	
	≥60 y	28	25.93	
BMI group	<18.5 kg/m ²	7	6.48	
	18.5–24.9 kg/m ²	41	37.96	
	25–29.9 kg/m ²	28	25.93	
	≥30 kg/m ²	32	29.63	
		Mean (±SD)	Median	Min–Max
Age		47.51 (±16.35)	48	21–80
BMI		26.66 (±5.92)	25.7	16.1–41.4

Note: Total number (N) and percentage (%) of patients are given, with further information on the distribution of sex and body mass index (BMI). Mean values and standard deviation (SD), median, minimum (min) and maximum (max) values for age and BMI are presented.

repeated measurements. For comparing the EM values between the investigators, an ANOVA was performed. We regarded p -values as significant at $p < 0.05$ without any adjustment for multiplicity.

RESULTS

Study population

The age groups of 20–40 y and 40–60 y consisted of 40 subjects each; the remaining group (>60 y) consisted of 28 subjects. Altogether, 64 subjects were women (59.3%). The mean age of all subjects was 47.5 y (SD = 16.35), with a median of 48 y. The mean BMI was 26.6 kg/m² (SD = 5.9), with a median of 25.7 kg/m². We found no significant differences in sex distribution within age groups ($\chi^2 = 0.5583$; $p = 0.76$). Furthermore, BMI did not correlate with age ($r = 0.10$, $p = 0.30$) or sex ($t = 0.43$, $p = 0.67$). No relevant correlations between possible confounders were found. Table 1 presents the characteristics of the study population.

Differences in shear wave elastography depending on age, sex, side of investigation and weight

The overall mean EM values were 3.34 kPa (SD = 0.59) on the left side and 3.33 kPa (SD = 0.58) on the right side. As the first, second and third measurements ($F = 1.09$, $p = 0.34$) and the measurements of left and right side ($F = 0.03$, $p = 0.87$) did not differ, we calculated a mean value of all repeated measurements of both sides.

We found no correlation between the EM values and BMI ($r = 0.07$, $p = 0.48$) or sex ($t = -0.11$, $p = 0.91$), but we did observe a significant correlation between the EM values and age ($r = 0.43$, $p < 0.0001$) (Fig. 1b). Results for age groups are displayed in Table 2 and Figure 1a.

Inter- and intra-rater reliability

All patients were investigated by three raters (rater 1 [n = 51], rater 2 [n = 43] and rater 3 [n = 14]). No significant differences concerning sex ($\chi^2 = 4.33$, $p = 0.11$) and BMI ($\chi^2 = 7.54$, $p = 0.27$) were found among patients investigated by the three raters, but there were significant differences concerning age groups ($\chi^2 = 9.69$, $p = 0.046$), as rater 1 investigated more of the older patients. Comparing the mean EM values of all measurements from both sides, we found no difference among the raters ($F = 0.46$, $p = 0.64$). Further information is presented in Figure 1c. Therefore, despite the variation in age distribution among raters, we conclude overall inter-rater reliability on elastography measurements.

Concerning intra-rater reliability we found no significant differences among the first, second and third measurements seen for rater 1 and 3. For rater 2, the second and third measurements on the right side differed significantly ($t = -2.06$, $p = 0.046$), as the mean of the second measurements was 3.15 kPa (SD = 0.91) and the mean of the third measurements was 3.54 kPa (SD = 1.04).

Comparison to measurements taken in patients with ischemic and hemorrhagic strokes

EM values of the ipsilateral side of patients with proof of ischemic stroke in neuroimaging were 1.58 and 2.35 kPa. One patient with proof of a hemorrhagic stroke showed an EM value of 10.98 kPa on the ipsilateral side. The values on the contralateral side were 3.49 and 4.72 and 3.57 kPa, respectively. As the patients were >60 y old, their EM values were compared with the mean value of the respective age matched patients (Tab. 3).

Statistical comparison was not reasonable because of the small number of patients. For illustration, values are given in Table 3 and Figure 1d. Pictures of uBPE and corresponding neuroimaging are presented in Figure 2.

DISCUSSION

The investigation of tissue stiffness using 2-D shear wave elastography is already widely used in clinical practice and research for a variety of parenchymatous organs, with the exception of the brain.

We determined in this study that brain tissue stiffness of the subcortical white matter can be safely and reliably measured, using the familiar transtemporal insonation approach. Values do not vary concerning sex and weight, for example, but are distinctly negatively related to age.

As far as we know from MR-elastography (MRE) studies, our values are in agreement with measurements in the deep white matter (average elasticity of 3.0 kPa [SD = 0.2] within the age group of 60–69 y). These values were also dependent on age in the same way as ours; the

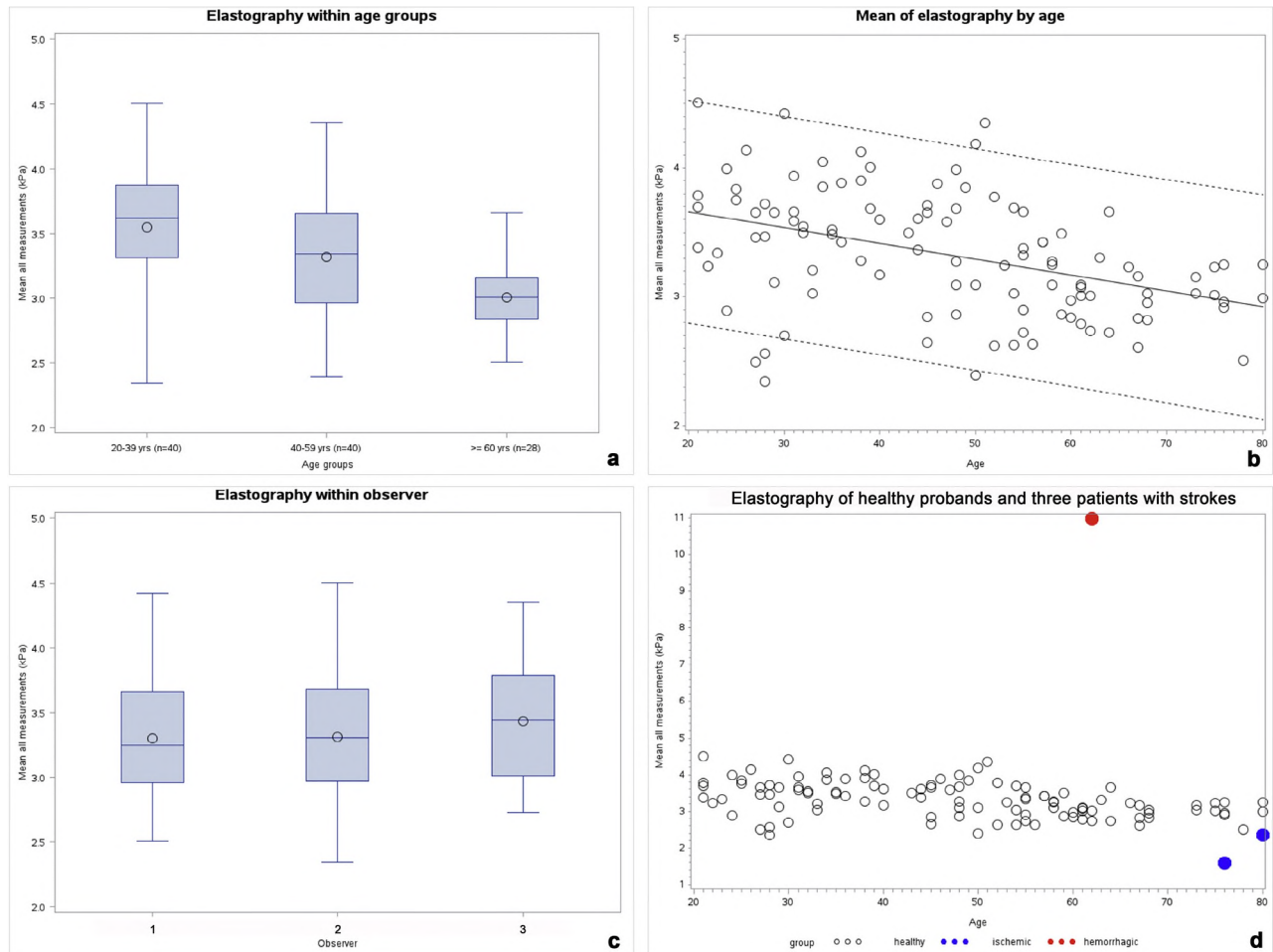


Fig. 1. (a) Elastography within age groups: mean values and standard deviations are presented. Significant differences could be detected between all age groups. (b) Distribution of the mean values of all measurements and prediction interval by age. Brain parenchyma elasticity decreases with age. (c) Boxplots with mean values and quantiles of all measurements sorted by observers. (d) Elastography of all patients and three exemplary patients: healthy patients (*white dots*), ischemic stroke patients (*blue dots*) and a patient with intra-cranial bleeding (*red dot*).

stiffness of occipital and temporal regions was also related to sex, with women having a higher tissue stiffness than men of the same age (Arani et al. 2015). Arani et al. (2015) detected an annual decline of 0.0011 kPa (SD = 0.002) in their population with a mean age of 74 y, ranging 60–89 y.

During aging, ultrastructural changes in white matter lead to a decrease in the structural matrix (extracellular matrix, microvasulature, membranes, etc.). The integrity of this matrix is important for shear wave propagation (Bamber et al. 2013) and leads to a progressive softening of brain tissue, resulting in decreased shear wave

Table 2. Differences in shear wave elastography between age groups

Age group	N	Mean	SD	Median	Min	Max	ANOVA		
							F	Coeff.	<i>p</i>
20–39	40	3.54	0.49	3.62	2.35	4.50	13.31	12.83	<0.0001
40–59	40	3.32	0.46	3.34	2.39	4.35			
≥60	28	3.00	0.24	3.01	2.51	3.66			
All	108	3.32	0.47	3.28	2.35	4.50			

Note: Mean values, standard deviation (SD), median, minimum (min) and maximum (max) values, sorted by age groups. F- and *p*- values and coefficient of variation are presented. Significant differences could be detected between all age groups.

Table 3. Comparison of measurements taken in patients with ischemic and hemorrhagic strokes to matched healthy patients

	Mean \pm SD (95%-CI)	
Healthy ≥ 60 (n = 28)	3.00 \pm 0.24 (2.91–3.10)	
	Ipsilateral side	Contralateral side
Hemorrhagic patient	10.98	3.57
Ischemic patient 1	1.58	3.49
Ischemic patient 2	2.35	4.72

Note: Elastography values in patients with hemorrhagic and ischemic strokes compared with the mean value of the respective aged matched patients. Mean values, standard deviation (SD) and 95%-confidence interval are presented.

velocity. Another aspect might be the absorption of parts of the shear wave stimulus by the skull bone. Older age and female sex are associated with an insufficient bone window mainly because of increased bone thickness (Wijnhoud et al. 2008). Arguments against a relevant

influence of this aspect are similar age dependent results from MRE and the requested immaculate bone window in the present study.

Because of the keyhole effect of transtemporal insonation, the range of brain regions to be investigated by uBPE is restricted and lacks the opportunity to analyze regions as the frontal lobes or the cerebellum, which is possible using MRE.

Apart from this, evidence on brain elastography remains scarce. Green et al. (2008) reported a mean white matter stiffness of 2.7 kPa, although they only investigated in a small group of five healthy men aged 23–61 y. Only few uBPE studies are available with the restriction to intra-operative measurements before brain tumor resection: Chauvet et al. (2016) measured surrounding normal brain tissue in addition to tumor entities, revealing a brain tissue stiffness of 7.3 kPa (SD = 2.1). These values are consistently higher than in our patient population for an obvious reason: Brain tissue adjacent to tumors is directly or indirectly compressed by the lesion itself or the surrounding edema.

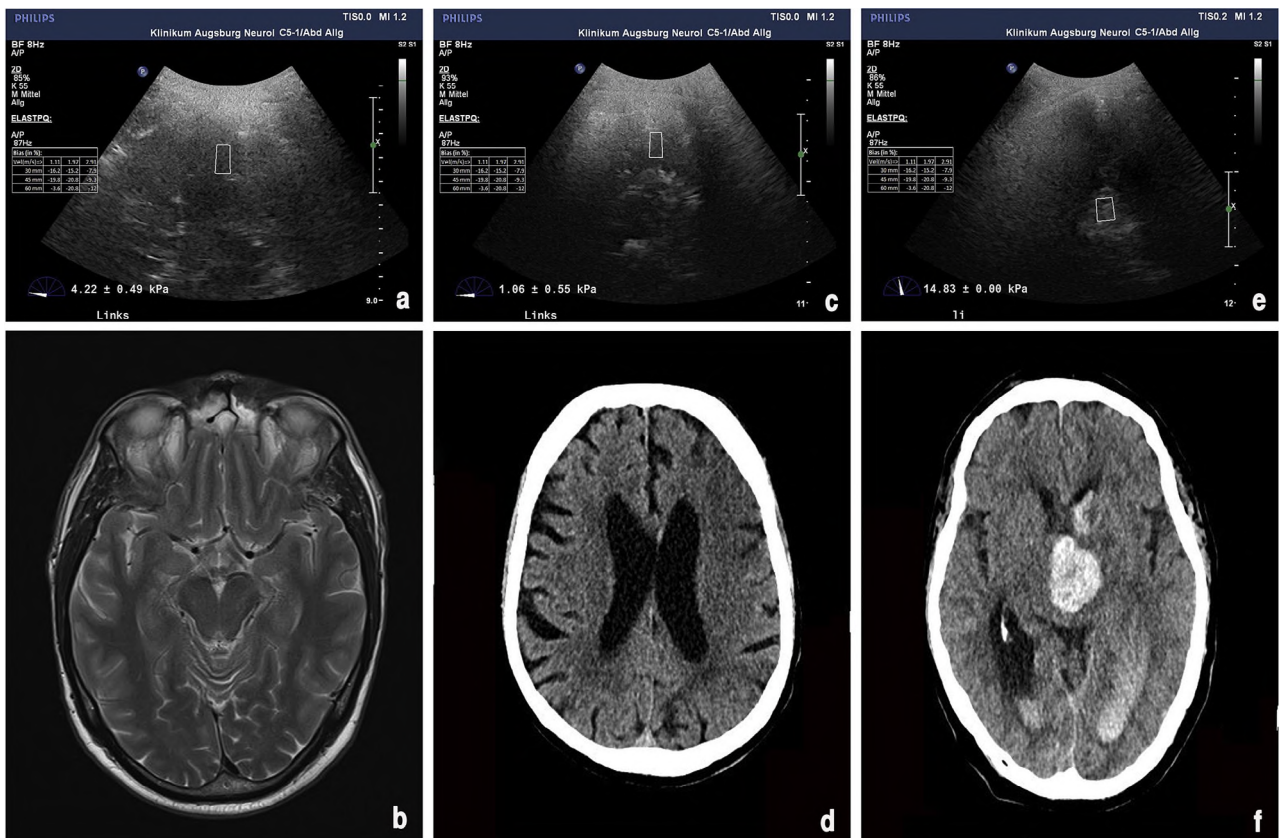


Fig. 2. Correspondence of ultrasound brain parenchyma elastography (uBPE) and conventional neuroimaging: (a, c, e) (a) Display of uBPE in a healthy subject; (b) patient with ischemic stroke of the left middle cerebral artery territory; (e), patient with a left hemispheric basal ganglia bleeding with connection to the cerebrospinal fluid compartment. (b, d, f) (b) Corresponding magnet resonance imaging (MRI) of a healthy volunteer; (d) computed tomography scan (CT) of a patient with ischemic stroke of the left middle cerebral artery territory; (f) CT scan of a patient with a left hemispheric basal ganglia bleed connecting to the cerebrospinal fluid compartment.

Based on the hypothesis that the effect of necrosis and edema—in line with findings in other tissues (Kuroiwa et al. 1997; Tanter et al. 2008)—following ischemic stroke leads to a reduced tissue stiffness within the lesion. This effect was investigated in an experimental animal model with artificial middle cerebral artery (MCA) occlusion. In comparison with control animals, the shear modulus was significantly reduced in the ischemic area. Possibly because of swelling effects and compression of the contralateral hemisphere, brain tissue stiffness was increased 24 h after lesion onset (Xu et al. 2013). As described in our exemplary patients with large ischemic hemispheric strokes, similar observations were reproducible: Brain tissue stiffness on the side of the lesion was reduced to age-matched normal values, whereas the stiffness on the contralateral side was increased. Both patients had a subtotal MCA infarction with midline shift, proven by neuroimaging.

Data on the behavior of blood properties investigated by elastographic imaging techniques are not available. A PubMed search using the key words *elastography*, *blood* or *bleeding* revealed no appropriate match. Nevertheless, it seems plausible, as blood has a higher density than parenchymatous tissues, that it might have an increased stiffness compared with normal tissue. Regions with visible blood in neuroimaging investigated in one of our patients had a significantly increased shear wave modulus.

The distinct difference of values taken in normal tissue and in areas affected by ischemic or hemorrhagic stroke might disclose an innovative and promising application of ultrasound elastography. Other possible applications might be the differential diagnosis of dementias or the identification of symptomatic lesions for epilepsy (temporal sclerosis), thereby complementing other imaging techniques (*e.g.*, CT, MRI) with all the advantages of ultrasound applications (bedside method, easily repeatable, *etc.*) Future studies should deal with the examination of aforementioned patient cohorts and correlation with MRE values.

Study limitations

The uBPE measurements were only taken in a previously standardized region of the deep white matter because of the limited access of transtemporal ultrasound. Other regions of the brain show slightly different shear wave modulations in MRE (Arani et al. 2015). On the other hand, the examined region comprises a large variety of possible affections as hemorrhagic or ischemic strokes, microangiopathy, degenerative and inflammatory lesions, disclosing a variety of possible clinical applications. Each patient was only investigated by one person, not allowing direct interrater comparisons. Still, values generated by the investigators showed a solid reliability in very similar patients.

CONCLUSIONS

Transtemporal uBPE is a valid, reproducible and investigator independent method to reliably determine brain parenchyma stiffness of the subcortical white matter in the presence of a definable transtemporal bone window. Values correspond accurately with those reported from animal research and MRE investigations and are not inferior to ultrasound measurements taken intra-operatively with direct contact to brain surface.

Normal values should be evaluated in additional studies. Such values could serve as a reference for studies on a variety of brain lesions, such as ischemic or hemorrhagic strokes, brain tumors or other forms of space-occupying intra-cranial lesions.

REFERENCES

- Arani A, Murphy MC, Glaser KJ, Manduca A, Lake DS, Kruse SA, Jack CR, Jr., Ehman RL, Huston J, 3rd. Measuring the effects of aging and sex on regional brain stiffness with MR elastography in healthy older adults. *Neuroimage* 2015;111:59–64.
- Bamber J, Cosgrove D, Dietrich CF, Fromageau J, Bojunga J, Calliada F, Cantisani V, Correas JM, D'Onofrio M, Drakonaki EE, Fink M, Friedrich-Rust M, Gilja OH, Havre RF, Jenssen C, Klausner AS, Ohlinger R, Saftoiu A, Schaefer F, Sporea I, Piscaglia F. EFSUMB guidelines and recommendations on the clinical use of ultrasound elastography. Part 1: Basic principles and technology. *Ultraschall Med* 2013;34:169–184.
- Barr RG, Cosgrove D, Brock M, Cantisani V, Correas JM, Postema AW, Salomon G, Tsutsumi M, Xu HX, Dietrich CF. WFUMB guidelines and recommendations on the clinical use of ultrasound elastography: Part 5. Prostate. *Ultrasound Med Biol* 2017;43:27–48.
- Barr RG, Nakashima K, Amy D, Cosgrove D, Farrokh A, Schafer F, Bamber JC, Castera L, Choi BI, Chou YH, Dietrich CF, Ding H, Ferraioli G, Filice C, Friedrich-Rust M, Hall TJ, Nightingale KR, Palmeri ML, Shiina T, Suzuki S, Sporea I, Wilson S, Kudo M. WFUMB guidelines and recommendations for clinical use of ultrasound elastography: Part 2: Breast. *Ultrasound Med Biol* 2015;41:1148–1160.
- Chauvet D, Imbault M, Capelle L, Demene C, Mossad M, Karachi C, Boch AL, Gennisson JL, Tanter M. *In vivo* measurement of brain tumor elasticity using intraoperative shear wave elastography. *Ultraschall Med* 2016;37:584–590.
- Cosgrove D, Barr R, Bojunga J, Cantisani V, Chammas MC, Dighe M, Vinayak S, Xu JM, Dietrich CF. WFUMB guidelines and recommendations on the clinical use of ultrasound elastography: Part 4. Thyroid. *Ultrasound Med Biol* 2017;43:4–26.
- Enzinger C, Barkhof F, Ciccarelli O, Filippi M, Kappos L, Rocca MA, Ropele S, Rovira A, Schneider T, de Stefano N, Vrenken H, Wheeler-Kingshott C, Wuerfel J, Fazekas F. MAGNIMS study group. Nonconventional MRI and microstructural cerebral changes in multiple sclerosis. *Nat Rev Neurol* 2015;11:676–686.
- Ferraioli G, Filice C, Castera L, Choi BI, Sporea I, Wilson SR, Cosgrove D, Dietrich CF, Amy D, Bamber JC, Barr R, Chou YH, Ding H, Farrokh A, Friedrich-Rust M, Hall TJ, Nakashima K, Nightingale KR, Palmeri ML, Schafer F, Shiina T, Suzuki S, Kudo M. WFUMB guidelines and recommendations for clinical use of ultrasound elastography: Part 3: Liver. *Ultrasound Med Biol* 2015;41:1161–1179.
- Garra BS, Cespedes EI, Ophir J, Spratt SR, Zurbier RA, Magnant CM, Pennanen MF. Elastography of breast lesions: Initial clinical results. *Radiology* 1997;202:79–86.
- Green MA, Bilston LE, Sinkus R. *In vivo* brain viscoelastic properties measured by magnetic resonance elastography. *NMR Biomed* 2008; 21:755–764.

- Kuroiwa T, Ueki M, Ichiki H, Kobayashi M, Suemasu H, Taniguchi I, Okeda R. Time course of tissue elasticity and fluidity in vasogenic brain edema. *Acta Neurochir Suppl* 1997;70:87–90.
- Li C, Zhang C, Li J, Cao X, Song D. An experimental study of the potential biological effects associated with 2-d shear wave elastography on the neonatal brain. *Ultrasound Med Biol* 2016;42:1551–1559.
- Sandrin L, Fourquet B, Hasquenoph JM, Yon S, Fournier C, Mal F, Christidis C, Ziol M, Poulet B, Kazemi F, Beaugrand M, Palau R. Transient elastography: A new noninvasive method for assessment of hepatic fibrosis. *Ultrasound Med Biol* 2003;29:1705–1713.
- Sarvazyan A, Hall TJ, Urban MW, Fatemi M, Aglyamov SR, Garra BS. An overview of elastography—An emerging branch of medical imaging. *Curr Med Imaging Rev* 2011;7:255–282.
- Shiina T, Nightingale KR, Palmeri ML, Hall TJ, Bamber JC, Barr RG, Castera L, Choi BI, Chou YH, Cosgrove D, Dietrich CF, Ding H, Amy D, Farrokh A, Ferraioli G, Filice C, Friedrich-Rust M, Nakashima K, Schafer F, Sporea I, Suzuki S, Wilson S, Kudo M. WFUMB guidelines and recommendations for clinical use of ultrasound elastography: Part 1: Basic principles and terminology. *Ultrasound Med Biol* 2015;41:1126–1147.
- Shiroishi MS, Cen SY, Tamrazi B, D'Amore F, Lerner A, King KS, Kim PE, Law M, Hwang DH, Boyko OB, Liu CS. Predicting meningioma consistency on preoperative neuroimaging studies. *Neurosurg Clin N Am* 2016;27:145–154.
- Su Y, Ma J, Du L, Xia J, Wu Y, Jia X, Cai Y, Li Y, Zhao J, Liu Q. Application of acoustic radiation force impulse imaging (ARFI) in quantitative evaluation of neonatal brain development. *Clin Exp Obstet Gynecol* 2015;42:797–800.
- Tanter M, Bercoff J, Athanasiou A, Deffieux T, Gennisson JL, Montaldo G, Muller M, Tardivon A, Fink M. Quantitative assessment of breast lesion viscoelasticity: Initial clinical results using supersonic shear imaging. *Ultrasound Med Biol* 2008;34:1373–1386.
- Toms DA. The mechanical index, ultrasound practices, and the ALARA principle. *J Ultrasound Med* 2006;25:560, 1; author reply 561–562.
- Vorlander C, Wolff J, Saalabian S, Lienenluke RH, Wahl RA. Real-time ultrasound elastography—a noninvasive diagnostic procedure for evaluating dominant thyroid nodules. *Langenbecks Arch Surg* 2010;395:865–871.
- Wang D, Hui SC, Shi L, Huang WH, Wang T, Mok VC, Chu WC, Ahuja AT. Application of multimodal MR imaging on studying Alzheimer's disease: A survey. *Curr Alzheimer Res* 2013;10:877–892.
- Wijnhoud AD, Franckena M, van der Lugt A, Koudstaal PJ, Dippel ED. Inadequate acoustical temporal bone window in patients with a transient ischemic attack or minor stroke: Role of skull thickness and bone density. *Ultrasound Med Biol* 2008;34:923–929.
- Xu W, Shi J, Zeng X, Li X, Xie WF, Guo J, Lin Y. EUS elastography for the differentiation of benign and malignant lymph nodes: A meta-analysis. *Gastrointest Endosc* 2011;74:1001–1009, quiz 1115.e1–4.
- Xu ZS, Lee RJ, Chu SS, Yao A, Paun MK, Murphy SP, Mourad PD. Evidence of changes in brain tissue stiffness after ischemic stroke derived from ultrasound-based elastography. *J Ultrasound Med* 2013;32:485–494.